European Journal of Medicinal Chemistry 215 (2021) 113276

Contents lists available at ScienceDirect

European Journal of Medicinal Chemistry

journal homepage: http://www.elsevier.com/locate/ejmech

Preparation and *in vitro* evaluation of amphiphilic paclitaxel small molecule prodrugs and enhancement of oral absorption

Yuanyuan Li [a, 1], Min Yang [a, 1], Yanli Zhao [d], Lingbing Li [a, **], Wei Xu [b, c, *]

[a] Department of Pharmaceutics, Key Laboratory of Chemical Biology (Ministry of Education), School of Pharmaceutical Sciences, Cheeloo College of Medicine, Shandong University, 44 Wenhuaxi Road, Jinan, Shandong Province, 250012, China
[b] Shandong Provincial Qianfoshan Hospital, The First Hospital Affiliated with Shandong First Medical University, China
[c] Shandong Provincial Qianfoshan Hospital, Shandong University, China
[d] Shandong Mental Health Center, Jinan, Shandong Province, China

ARTICLE INFO

Article history:
Received 14 December 2020
Received in revised form
1 February 2021
Accepted 2 February 2021
Available online 6 February 2021

Keywords:
Paclitaxel
Small molecule prodrug
Oral administration
Transporter PEPT1

ABSTRACT

A series of novel amphiphilic paclitaxel (PTX) small molecule prodrugs, PTX-succinic anhydride-cystamine (PTX-Cys), PTX-dithiodipropionic anhydride (PTX-SS-COOH) and PTX-succinic anhydride-cystamine-valine (PTX-SS-Val) were designed, synthesized and evaluated against cancer cell lines. Compared with paclitaxel, these prodrugs contained water-soluble groups such as amino, carboxyl and amino acid, which improved the aqueous solubility of the prodrugs. More importantly, the valine was introduced in PTX-SS-Val molecule and made the molecule conform to the structural characteristics of intestinal oligopeptide transporter PEPT1 substrate. Thus the oral bioavailability of prodrug could be improved because of the mediation of PEPT1 transporter. These small molecule paclitaxel prodrugs could self-assemble into nanoparticles in aqueous solution, which effectively improved the solubility of paclitaxel, and had certain stability in pH 6.5, pH 7.4 buffer solutions and simulated gastrointestinal fluids. Some of these prodrugs, especially for PTX-Cys and PTX-SS-Val, exhibited nearly equal or slightly better anticancer activity when compared to paclitaxel. Further studies on PTX-Cys and PTX-SS-Val showed that both had good intestinal absorption in the rat single-pass intestinal perfusion (SPIP) experiments. Oral pharmacokinetic experiments showed that PTX-SS-Val could effectively improve the oral bioavailability of PTX.

1. Introduction

Paclitaxel (PTX) is a microtubule inhibitor with a highly effective anti-tumor effect and is a clinical first-line chemotherapeutic drug, which is effective against a broad range of solid tumors, including refractory ovarian cancer, metastatic breast cancer, non-small-cell lung cancer, AIDS-related Kaposi's sarcoma, head and neck malignancies and other cancers [1]. However, the clinical utilization of PTX is primarily limited by poor solubility (0.3–0.5 μg/mL) and low membrane permeability [2]. At present, most marketed PTX formulations are administered by intravenous injection, which has poor patient adherence, severe toxic side effects associated with excipients. For example, clinically, PTX is currently dissolved in a 50/50 (v/v) mixture of Cremophore EL/dehydrated ethanol as commercial Taxol® or Paxene®, which is further diluted in isotonic saline solution before intravenous (i.v.) administration. Unfortunately, i.v. administration of the current Cremophore EL-based formulation in a non-aqueous vehicle may lead to serious side effects in some patients such as hypersensitivity, neurotoxicity, nephrotoxicity, and precipitation on aqueous dilution [3]. Based on the above problems, there is a need for the development of alternative formulations of PTX to solve these problems.

Oral administration is more flexible, safe and convenient. Compared with intravenous injection, oral administration is a much more preferable choice for PTX. It shows better patient compliance, less cost and more chronic treatment regimen. However, as a result of the poor solubility (0.25 mg/mL) and low permeability across the intestinal barrier, the oral bioavailability of

* Corresponding author. Shandong Provincial Qianfoshan Hospital, the first Hospital Affiliated with shandong First Medical University, China.
** Corresponding author. Department of Pharmaceutics, School of Pharmaceutical Sciences, Shandong University, Jinan, Shandong Province, 250012, China.
E-mail addresses: cnlbli@email.sdu.edu.cn (L. Li), 13964016747@126.com (W. Xu).
[1] The first two authors contributed equally to this study.

https://doi.org/10.1016/j.ejmech.2021.113276
0223-5234/

PTX is less than 10% [4]. For example, the first-pass effect of the gastrointestinal tract and the affinity of drugs to efflux proteins (P-glycoproteins) are the main factors affecting oral bioavailability [5]. Thus, the design of PTX small molecular prodrugs to improve the solubility and permeability across the intestinal barrier is preferable choice. Among the numerous drug transporters in the intestine, oligopeptide transporter (PEPT1) is one of the important targets in the design of oral targeted prodrugs because of its substrate structure specificity, high expression and transport capacity. PEPT1 is mainly expressed in small intestinal epithelial cells and has higher protein activity. PEPT1 substrates are mainly dipeptides, tripeptides and their analogues produced by protein hydrolysis [6]. Peptide-mimetic derivatives formed by drug-amino acid linkage can also serve as PEPT1 substrates. In addition, as the demand for nutrients in malignant proliferation of tumors increases, the L-type amino acid transporter 1 (LAT1) of tumor cells are more highly expressed than normal cells which can be used as targets for active targeting of cancer [7]. Tao et al. found that modified by PEPT1 substrate, L-valine, the oral bioavailability of cytarabine prodrug, 5′-valine-cytarabine, in rats was increased to 60% compared with cytarabine (20.8%), which is why the clinical trial of 5′-valine cytarabine was approved by CFDA [8]. These studies show that using PEPT1 targeted amino acid prodrugs can effectively improve the oral bioavailability of drugs.

In recent years, amphiphilic small molecule prodrug based systems have shown significant advantages in cancer treatment and disease diagnosis. Through chemical modification of the parent drug, we can improve the solubility and stability of the drug, improve the distribution in the body and the permeability of biological membranes. Also avoiding or reducing the use of polymeric carrier materials in the formulation, we can reduce toxicity and improve biosafety effectively [9]. Many researchers combined hydrophobic drugs with hydrophilic or hydrophobic organic molecules, such as polymer chains [10], peptides [11], fluorescent substances [12], drug molecules [13], phospholipids or DNA/antibodies [14–16], to form amphiphilic small molecule prodrug that can self-assemble into nanoparticles in aqueous solution. Through this way, the shortcomings of parent drugs as described above could be largely overcome. Most of the small molecule prodrugs were designed to overcome paclitaxel's low water solubility or increase the targeting ability of paclitaxel. Hydrophilic molecules such as carboxylic acids, phosphates, sulfonates, amines, or polyethylene glycol, sugar, etc. have been exploited as backbones for PTX prodrugs, resulting in significantly improved water solubility [17]. However, because of the high hydrophilicity, most prodrugs were faced with poor cell uptake or intracellular process [18]. The other way for the small molecule paclitaxel prodrug was to make paclitaxel with hydrophobic moiety. These hydrophobic paclitaxel prodrugs were more suitable for nanoparticle drug delivery systems, which could increase the accumulation in tumor tissues because of enhanced permeability and retention effect (EPR effect) of nanoparticles [19]. However, high-level tumor accumulation of nanoparticles does not directly correlate to the clinical efficacy, which is more dependent on the rate of drug released [20].

As can be found in literature, modifying drugs or drug loaded carriers with some positively charged groups or groups with tendency of ionization in specific biological microenvironment can effectively promote the permeability of drugs or carriers across cell membrane, which provides new ideas for designing tumor specific drugs or drug loaded carriers [21]. Zhou and co-workers developed amphiphilic poly-2-(l-γ-glutamylamino) ethyl acrylamide (PEAGA)-Camptothecin based enzyme sensitive polymeric micelles for delivering camptothecin. The overexpressed γ-glutamyl transpeptidase on the tumor cell membrane cleaved the γ-glutamyl moieties of the conjugate to generate positively charged primary amines, which resulted in significantly increased tumor penetration of the conjugate [22]. Thus, application of positively charged delivery systems can thereby promote the uptake of tumor cells and intestinal absorption.

In order to realize responsive release at tumor sites, chemical groups sensitive to external magnetic field, temperature, ultrasound, light, current and physiological signals (enzyme, pH, Redox potential) have been widely used in drug delivery system design [23]. It has been reported that there is a significant difference in reduced glutathione (GSH) concentration between the extracellular and intracellular tumor microenvironment, enabling prodrugs containing disulfide bonds to effectively release the parent drugs in tumor cells and exert better therapeutic efficacy [24].

In this work, a redox-responsive small molecular PTX prodrug containing a disulfide bond, PTX-succinic anhydride-cystamine (PTX-Cys) with an exposed amino group, was successfully synthesized. The exposed dissociable amino group could improve the solubility and dispersion of PTX in aqueous solution and the disulfide bonds could be degraded in highly reductive tumor micro or intracellular environment to promote the PTX release in tumor tissues. Based on this, a novel type of prodrug was developed. PTX-Cys and PEPT1 substrate, L-valine (Val), were linked by amide bonds and the prodrug, PTX-succinic anhydride-cystamine-Valine (PTX-SS-Val), was synthesized. It can be predicted that this prodrug could be mediated by PEPT1 transporter to across the intestinal cell membrane and the oral bioavailability of paclitaxel could be effectively improved. In addition, PTX-dithiodipropionic anhydride (PTX-SS-COOH) with an exposed carboxyl group was also successfully synthesized as a control. The exposed dissociable carboxyl group could improve the solubility and dispersion of PTX in aqueous solution and the disulfide bonds could be degraded in highly reductive tumor micro or intracellular environment to promote the PTX release in tumor tissues. To test the effect of different prodrugs on the membrane permeability and inhibition efficiency of tumor cells, the cytotoxicity and cell uptake test of the PTX prodrugs at cellular level were measured and the mechanism was investigated. Furthermore, the effects of prodrugs on intestinal absorption and transmembrane transport were studied in rats. Animal experiments have proved that the transporter PEPT1 can realize the transmembrane transport of intestinal cells through PEPT1 mediated transport of PTX-SS-Val, effectively improving the oral bioavailability of paclitaxel.

2. Materials and methods

2.1. Materials

PTX was obtained from Mellon, Dalian, China; Succinic Anhydride (SA), Cystamine Dihydrochloride (Cys), Dithiodipropionic (DTDP), Boc-L-Valine (Val), 1-hydroxybenzotriazole (HOBT), 1-(3-dimethylaminopropyl)-3-ethyl carbonimide hydrochloride (EDCI), Tween 80, Dichloromethane (DCM) were all purchased from Aladdin, Shanghai, China; 3-(4,5-dimethylthiazole-2)-2,5-diphenyltetrazolium bromide (MTT), Dialysis bag (MWCO500D), Pepsin, Trypsin, AnnexinV-FITC/PI apoptosis detection kit were all obtained from Solarbio, Beijing, China; Glycyl-Sarcosine (Gly-Sar) was purchased from Xianding Biology, Shanghai, China; Other solvents were supplied by Zhaoxu, Jinan, China and Fuyu, Tianjin, China.

Human breast cancer (MCF-7) cells were obtained from Institute of Immunopharmacology, Shandong University School of Pharmacy. Male Wistar Rats were supplied by Medical Animal Test Center of the New Drugs Evaluation Center, Shandong University.

2.2. Synthesis of PTX-Cys, PTX-SS-Val and PTX-SS-COOH

2.2.1. Synthesis of PTX-Cys

The small molecule prodrug, PTX-Cys, was obtained by amidation of PTX-Succinic anhydride conjugate (PTX-COOH) (see supporting information) and cystamine. PTX-COOH (50 mg, 0.05 mmol), EDCI (15 mg, 0.078 mmol), HOBT (10.5 mg, 0.078 mmol) were dissolved in DMF and stirred at 0 °C for 6 h under nitrogen atmosphere. Additionally, cystamine hydrochloride (35.5 mg, 0.158 mmol) and TEA (48 μl) were dissolved in DMF under ultrasound for 2 h and mixed with above low-temperature solution. The reaction was proceeded for 24 h at 25 °C. The resulting solution was added into ice water, the product was precipitated, centrifuged (8000 rpm, 5 min). The supernatant was discarded and the precipitate was lyophilized, and purified by column chromatography (dichloromethane-methanol system) to obtain PTX-Cys. The structure of PTX-Cys was confirmed by ^{1}H NMR (solvent: deuterated DMSO, DMSO-d_6), FT-IR and MS.

2.2.2. Synthesis of PTX-SS-Val

The small molecule prodrug PTX-SS-Val was obtained by amidation of PTX-Cys and L-valine. Boc-L-valine (20 mg, 0.092 mmol), EDCI (26.5 mg, 0.138 mmol), HOBT (18.6 mg, 0.138 mmol) were dissolved in DMF, stirred at 0 °C for 6 h under nitrogen atmosphere, and then 50 mg of PTX -Cys was added into the solution to proceed for additional 24 h. The resulting solution was added to ice water, the product was precipitated, centrifuged (8000 rpm, 5 min), and the supernatant was discarded to remove water-soluble impurities. An appropriate amount of ethyl acetate was added to extract the product. The organic phase was mixed and a small amount of anhydrous sodium sulfate was added to dry overnight. The product was stirred in dichloromethane (DCM) solution containing 15% TFA at room temperature for 2 h, the protective group of Boc-L-valine was removed [25], and the reaction progress was monitored by thin layer chromatography (TLC). After the reaction, the solvent was removed by vacuum rotary evaporation method, and the crude product was purified by column chromatography (dichloromethane-methanol system) to obtain PTX-SS-Val. The structure of PTX-SS-Val was confirmed by ^{1}H NMR (solvent: deuterated DMSO, DMSO-d_6) and FT-IR.

2.2.3. Synthesis of PTX-SS-COOH

PTX-SS-COOH was synthesized with methods reported previously. Briefly, PTX-SS-COOH was synthesized by esterification of DTDPA (see supporting information) and 2'-OH of Paclitaxel. The mixture of PTX (0.030 g, 0.035 mmol), DTDPA (0.067 g, 0.35 mmol) and dimethylaminopyridine (DMAP, 0.034 g, 0.29 mmol) in pyridine was stirred under nitrogen atmosphere below 35 °C for 24 h. The system was concentrated through rotary evaporation under reduced pressure and 1% (m/V) HCl solution was added to take away residual pyridine. Product in aqueous phase was extracted with DCM three times and the organic phase was collected. The organic solvent was removed and dried in vacuum overnight. The product was characterized with ^{1}H NMR, FT-IR and MS.

2.3. Preparation and characterization of paclitaxel prodrug nanoparticles

2.3.1. Preparation of paclitaxel prodrug nanoparticles

The nanoparticles of PTX prodrugs were prepared by nanoprecipitation method. 1 mg of PTX prodrug was precisely weighed and dissolved in 1 mL methanol and added dropwise into 5 mL deionized water under stirring. The organic solvent was volatilized by stirring, and the solution was transferred to a dialysis bag (MWCO500D) for dialysis against deionized water for 24 h.

2.3.2. Measurement of appearance and size distribution of nanoparticles

The appearance of PTX prodrug nanoparticles was observed by transmission electron microscopy (TEM, JEM-100SX, Japan). A drop of solution was placed on a copper grid for TEM and the excess fluid was absorbed with a piece of filter paper from the edge of the copper disk. Before observation, copper grid containing sample solution was immediately stained with a drop of phosphotungstic acid (2 wt% aqueous solution) for 30 s.

The particle size and size distribution of PTX-Cys, PTX-SS-Val and PTX-SS-COOH nanoparticles were measured by a laser particle size analyzer (Malvern, U.K.).

2.4. In vitro stability of PTX prodrugs

2.4.1. Investigation of chemical stability of PTX prodrugs in buffer solutions

The dialysis method was employed to study the stability of PTX prodrugs in disodium hydrogen Phosphate-Citric acid buffer (pH 7.4 and 6.5) containing 0.5% Tween 80. The PTX release in buffer solution in pH 6.5 with or without dithiothreitol (DTT) (10 mM) was also measured to evaluate the redox stability of prodrugs. Briefly, an appropriate amount of prodrug (2.5 mg PTX) was weighed and dissolved in the above three buffer solutions (pH 6.5, pH 7.4, pH 6.5 containing DTT) and diluted to 6 mL. 2 mL of the above solution was moved into the dialysis bag (MWCO = 1000, n = 3), and then the bag was put into a centrifuge tube filled with 35 mL same buffer solution and shaken in a water bath at 37 °C, 100 rpm. At predetermined interval (1, 2, 4, 8, 12, 24, 36, 48, 72, 96, 120 h), 1 mL of release medium was removed from centrifuge tube to determine the PTX content and 1 mL corresponding isothermal buffer solution was supplemented.

The PTX content was measured by high performance liquid chromatography (HPLC) at 227 nm (Elite Hypersil ODSC18 4.6 × 250 mm, 5 μm particle size). The mobile phase consisted of acetonitrile: water = 50:50 (v/v), and the flow rate was 1 mL/min, the injection volume was 20 μL, the column temperature was room temperature [26]. The cumulative release of PTX was further calculated according to the standard curve to investigate the stability of PTX prodrug in three buffer solutions.

2.4.2. Investigation on the stability of PTX prodrugs in simulated gastric (SGF) and intestinal fluid (SIF)

The stability of PTX prodrugs in SGF and SIF (contains 0.5% Tween 80) was investigated by dialysis bag method same as 2.4.1. According to the time rule of human gastric emptying and intestinal emptying, 1 mL of SGF was sampled at 0, 2, 4 h, and 1 mL of SIF was sampled at 0, 2, 4, 6, 8, 12 h, and fluid was replenished at same time. By HPLC, the sample concentrations at different time points were determined and calculated according to the standard curve, and the cumulative release of PTX was further calculated to investigate the stability of PTX prodrugs in simulated gastric and intestinal fluid.

2.5. Cytotoxicity experiments

In this section, cytotoxicity of Taxol®, PTX, PTX-Cys, PTX-SS-Val and PTX-SS-COOH solutions was evaluated with MTT assay. MCF-7 cells in logarithmic phase were digested with trypsin, diluted with prepared DMEM medium to suitable cell density and transferred to 96-well plate at a density of 5000 cells/well. Cells were incubated overnight till cells were in adherent growth for experiment and then blank medium was substituted with filtered solution containing different concentrations (0.1, 0.5, 1, 5, 10 g/mL) of Taxol®, PTX, PTX-Cys, PTX-SS-Val and PTX-SS-COOH (dissolved in

DMSO and diluted by medium), in which sterile DMSO was below 1‰. Cell viability was measured by MTT assay. Each concentration was repeated for five times, and negative control group (just medium, no cells and formulations) and positive control group (cells, medium, but no formulations) were set. The 96-well plate was incubated for 48 h and washed three times by PBS. 20 μL of MTT solution (5 mg/mL) was added into each well and incubated for additional 4 h. Thereafter, the medium was removed and 200 μL of DMSO was added to dissolve formazan crystals. The absorbance (OD) was measured by ELIASA at 570 nm and the cell viability was calculated.

2.6. Cell uptake experiments

In vitro cell uptake of three PTX prodrugs was evaluated by inverted fluorescence microscopy. Since PTX has no fluorescence, the fluorescent substance coumarin 6 (C6) was encapsulated in the hydrophobic core of three PTX prodrug nanoparticles by nanoprecipitation method in Ref. [27]. MCF-7 cells in logarithmic growth phase were seeded in 6-well plate at a density of 3×10^5 cells/well and cultured overnight. The cells were treated with C6-loaded prodrug nanoparticles for 4 h at a total drug concentration of 5 μg/mL and C6 at the concentration of 2 μg/mL. The cells were washed three times with cold PBS and fixed with 4% paraformaldehyde solution for 20 min at 4 °C in darkness. After drawing away paraformaldehyde solution, cells were washed 5 times with PBS buffer solution (pH 7.4) and the nuclei of cells were stained with 100 μl DAPI solution (10 μg/mL) for 20 min in a dark environment with 5% CO_2 at 37 °C.Finally, the cells were observed under fluorescent microscope (OLYMPUS, Tokyo, Japan).

2.7. Cell apoptosis analysis

Apoptotic experiments were performed by inverted fluorescence and flow cytometry, in which changes in the nucleus could be observed under inverted fluorescence microscopy, and apoptosis could be quantitatively detected by flow cytometry.

2.7.1. Inverted fluorescence microscopy

PTX, PTX-Cys, PTX-SS-Val and PTX-SS-COOH solutions with PTX concentration of 2.5 μg/mL were prepared respectively according to 2.5. MCF-7 cells in logarithmic growth phase were seeded in 12-well plate at a density of 1×10^5 cells/well and cultured overnight. The cells were treated with different sample solutions and each group of samples was repeated three times. MCF-7 cells in blank medium were set as a negative control group. The cells were incubated for 48 h respectively and washed with cold PBS three times. The other steps were the same as 2.6, and the morphological changes of the nucleus were finally observed under an inverted microscope.

2.7.2. Flow cytometry

The formulation solutions used to treat cells were the same as 2.7.1, and the operation steps were the same as 2.6. Apoptosis of PTX prodrugs was further quantified by flow cytometry using Annexin V-FITC/PI kit.

2.8. The absorption of small molecule prodrugs in the intestine

The oral absorption characteristics of PTX-Cys and PTX-SS-Val were preliminarily evaluated by single-pass intestinal perfusion (SPIP) in rats. The effects of pH value, different drug concentrations and different intestinal segments on intestinal absorption of drugs were investigated, and the intestinal absorption mechanisms of PTX-Cys and PTX-SS-Val were explored.

2.8.1. The single-pass intestinal perfusion (SPIP) in the intestine

This part of the test was carried out based on a reported method [28] and all the animal experiments were approved by the Shandong University Animal Care and Use Committee. Healthy male Wistar rats weighing 250 ± 20 g were fasted for approximately 12 h before the perfusion experiment with free access to water only. Anesthesia was induced by intraperitoneal injection of 10% chloral hydrate solution (0.34 g/kg). Then a midline abdominal incision was made and the experimental intestinal segment of approximately 8 cm was carefully exposed and cannulated at both ends. The exposed segment was covered with a piece of medical gauze soaked in normal saline. The body temperature of animals was maintained at 37 °C throughout the experiment using an infrared lamp. Both ends of the experimental intestinal segment were connected with a constant-flow pump. Warm saline passed slowly through the tract to clear the gut. After gut cleared, the PTX formulations, diluted in perfusion solution, were perfused circularly through the selected intestine at an entering flow rate of 0.20 mL/min. After 10 min of uniform circulation and 2 h of stable perfusion, the volume of perfusion solution in the measuring cylinder was recorded and 1 mL of perfusion solution sample was taken. At the end of the experiment, the rats were sacrificed by cervical dislocation. The length and inner diameter of each intestinal segment were measured. Each sample was repeated in three parallel groups.

2.8.2. Sample and data processing methods

Due to the polarity of prodrugs and the interference of perfusate components, the specificity of high performance liquid chromatography for detection of different PTX prodrugs is poor. Thus, according to Ref. [29], the prodrug in perfusate was hydrolyzed by HCl (3 M) at 85 °C for 2 h before measurement and PTX obtained was used as precursor to detect the change of PTX prodrug concentration in perfusate using the same method as described in 2.4.1. The apparent permeability coefficient (P_{eff}) and absorption flux (J) of prodrugs in each intestinal segment were calculated using the following equations [30]:

$$P_{eff} = -\frac{Q}{2\pi rl} \times In\left(\frac{C_{out} \times V_{out}}{C_{in} \times V_{in}}\right)$$

$$J = P_{eff} \times [C]$$

where C_{out} and C_{in} represent the concentration of tested compounds in the outlet and inlet perfusate, respectively (μg/mL); V_{out} and V_{in} are the outlet and inlet volume, respectively (mL). Q is the flow rate of entering solution (0.2 mL/min), while r is the intestinal radius and l is the intestinal length; $[C]$ is the logarithmic mean of C_{in} and C_{out} (μg/mL).

2.8.3. Effect of different pH on intestinal absorption

To investigate the effect of perfusate pH on intestinal absorption, pH 6.5 MES buffer and pH 7.4 HEPES buffer (70 mM NaCl, 2.7 mM KCl, 0.9 mM $CaCl_2$, 2.5 mM D-glucose, 12.5 mM MES or HEPES, NaOH and 0.5% Tween 80) were prepared and used to prepare solutions of PTX, PTX-Cys and PTX-SS-Val respectively (PTX concentrations were all 100 μg/mL). The single-pass intestinal perfusion (SPIP) of prodrug samples was performed in the jejunal segment for 2 h. The concentration of PTX was determined by HPLC as described in 2.8.2. Further, the apparent permeability coefficient (P_{eff}) of PTX, PTX-Cys and PTX-SS-Val was calculated respectively.

2.8.4. Effect of drug concentration on intestinal absorption

To investigate the effect of drug concentration on intestinal absorption, Kerbs-Ringer solution (67 mM NaCl, 2.4 mM KCl,

1.7 mM $CaCl_2$, 0.1 mM $MgCl_2$, 1.3 mM NaH_2PO_4, 8.1 mM $NaHCO_3$, 3.8 mM D-glucose and 0.5% Tween 80) was prepared and different formulations of PTX-Cys and PTX-SS-Val with different concentrations were prepared respectively using Kerbs-Ringer solution. The concentration gradients of PTX solutions were 70, 100, 120 and 150 μg/mL. The concentration of PTX prodrugs was determined by HPLC as described in 2.8.2. Further, the apparent permeability coefficient (P_{eff}) of PTX, PTX-Cys and PTX-SS-Val was calculated respectively.

In addition, following the end of the concentration-dependent experiment of PTX-SS-Val perfusion, the tested intestine segment was removed and washed with ice-cold saline. The tissue was then homogenized in a tissue homogenizer and diluted with isovolumetric saline solution. After centrifugation at 13000 rpm for 5 min, the supernatant was stored at −80 °C until analysis by HPLC.

2.8.5. The absorption of PTX prodrugs in the different intestinal segments

To explore the absorption of PTX, PTX-Cys and PTX-SS-Val in different intestinal segments, SPIP was conducted in duodenum, jejunum and ileum segments, respectively. PTX, PTX-Cys and PTX-SS-Val dissolved in above Kerbs-Ringer solution (PTX concentrations were all 100 μg/mL) were perfused through different intestinal segments respectively. The concentration of PTX prodrugs was determined by HPLC as described in 2.8.2. The apparent permeability coefficient (P_{eff}) of PTX, PTX-Cys and PTX-SS-Val in duodenum, jejunum and ileum was calculated respectively.

2.9. Investigation of the effect of inhibition PEPT1 on PTX-SS-Val transport

Gly-Sar is a classical substrate of the transporter PEPT1. In order to investigate the inhibition effect of Gly-Sar to PEPT1 mediation transport of PTX-SS-Val, the Gly-Sar was added in pH 7.4 HEPES solution (12.5 mM HEPES, 70 mM NaCl, 2.7 mM KCl, 0.9 mM $CaCl_2$, 2.8 mM glucose, 22.5 mM Gly-Sar and 0.5% Tween 80) and co-perfused with PTX and PTX-SS-Val (PTX concentration of 100 μg/mL) respectively. The concentration of PTX in both solutions was 100 μg/mL. The concentration of PTX and PTX-SS-Val was determined by HPLC as described in 2.8.2. The apparent permeability coefficient (P_{eff}) was calculated respectively.

2.10. Oral pharmacokinetic experiments

Male Wistar rats (weighing 250 ± 20 g) were fasted overnight with free access to water for 12 h before the experiment. The rats were divided randomly into two groups (n = 5) and administered Taxol® and PTX-SS-Val (containing 0.5% carboxymethyl cellulose and 1% Tween 80) at a dose of 25 mg/kg by intragastric administration respectively [31]. Taxol® was also administered intravenously to one group of rats at a dose of 6 mg/kg as a control. At predetermined times (0.25, 0.5, 1, 2, 4, 6, 8, 12 and 24 h), serial blood samples (0.2 mL) were collected from the orbital plexus, transferred to pretreated heparinized tubes and separated immediately by centrifugation (4000 rpm for 15 min). After centrifugation, the supernatant plasma obtained was stored at −20 °C until analysis.

The plasma protein was precipitated by adding a 1 mL mixture of methanol: acetonitrile = 1:1, vigorous vortex mixing for 5 min and centrifuging at 10000 rpm for 10 min. Each supernatant layer was transferred into another glass tube and evaporated under a gentle stream of nitrogen gas at 37 °C. The residues were reconstituted in 200 μL acetonitrile. 1 mL of 3 M hydrochloric acid was added, incubated at 85 °C for 2 h to hydrolyze them thoroughly, and then 0.85 mL of 0.5% ammonium carbonate (v/v) was added to terminate the reaction. The mixture was extracted with a large amount of ethyl acetate, and the organic phase was removed by rotary evaporation. Finally, the sample was reconstituted in 200 μL acetonitrile and the plasma concentrations of PTX in different formulations at different time points were detected by HPLC. Pharmacokinetic parameters were calculated using a non-compartmental model by DAS2.0 software, and the absolute bioavailability (F%) of PTX from different oral formulations was examined using the following equation:

$$F\% = \frac{AUC_{oral} \times D_{i.v.}}{AUC_{i.v.} \times D_{oral}} \times 100\%$$

where AUC_{oral} and $AUC_{i.v.}$ were the areas under the plasma concentration−time curve of PTX for the oral and intravenous administration, respectively; $D_{i.v.}$ and D_{oral} were the dosages of PTX for the intravenous and oral administration, respectively.

The PTX content was measured by the HPLC technique described above with an Agilent 1200 HPLC system consisting of a G1314B UV detector and a G1310A pump, equipped with a RP column (Elite Hypersil ODSC18 4.6 × 250 mm, 5 μm particle size) at 227 nm. The mobile phase consisted of acetonitrile: water = 50:50 (v/v), and the flow rate was 1 mL/min, the injection volume was 20 μL, the column temperature was room temperature.

2.11. Statistical analysis

Statistical evaluation was performed by one-way analysis of variance (ANOVA) using SPSS software (version 23.0). All the experiments were repeated at least three times, and the data were expressed as the mean ± standard deviation (S.D.), unless otherwise noted, $p < 0.05$ was considered statistically significant.

3. Results and discussions

3.1. Synthesis and characterization of PTX-Cys, PTX-SS-Val and PTX-SS-COOH

The synthesis procedures of PTX-Cys, PTX-SS-Val and PTX-SS-COOH were displayed in Fig. 1. The characterization of PTX-Succinic anhydride conjugate (PTX-COOH) was shown in Fig. S1. And the ^{1}H NMR of DTDP and DTDPA were shown in Fig. S2. The ^{1}H NMR and FT-IR spectra of the three target compounds were shown in Fig. 2 and Fig. 3, respectively.

PTX-Cys was obtained by amide reaction between the amino group of cystamine and the carboxyl group of PTX-COOH and the yield of PTX-Cys was 63.81%. The ^{1}H NMR, FT-IR spectra of PTX-Cys were shown in Figs. 2B and 3B. In the ^{1}H NMR spectrum of PTX-Cys (Fig. 2B), the hydrogen proton peaks attributed to PTX benzene ring appeared at 7.0−8.0 ppm, the characteristic peak attributed to cystamine appeared at 3.45 ppm, and the carboxyl peak of PTX-COOH at 12.18 ppm (Fig. S1) disappeared. Besides, the FT-IR spectrum of PTX-Cys (Fig. 3B) showed that the double absorption peaks of amino-linked methylene appeared at 2850.38 cm^{-1} and 2920.62 cm^{-1}, while the peak at 2800-3700 cm^{-1} attributed to carboxyl broad absorption of PTX-COOH disappeared (Fig. S1) and the characteristic absorption peak of PTX appeared at 707.67 cm^{-1}. Furthermore, the $[M+H]^+$ ion peak at m/z 1088.6 of PTX-Cys was confirmed by MS (Fig. S3A), suggesting that the cystamine was mono-substituted by PTX-COOH, which was consistent with the molecular weight of the designed mediates. The above results of ^{1}H NMR, FT-IR and MS spectra of PTX-Cys proved the successful synthesis of PTX-Cys.

PTX-SS-Val was obtained by amide reaction between the amino group of PTX-Cys and the carboxyl group of Boc-L-valine, after which the Boc protective group was removed, and the PTX-SS-Val

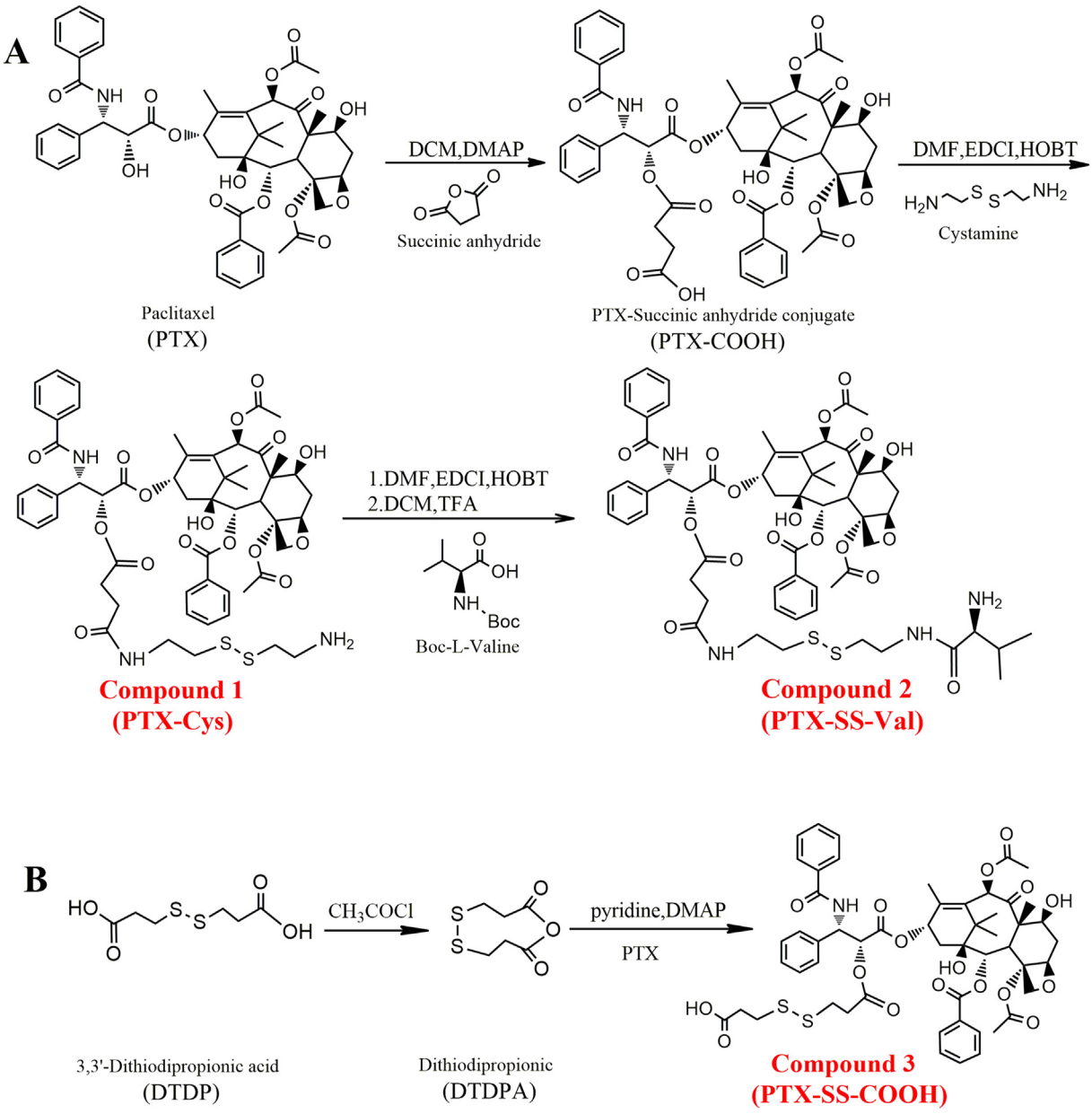

Fig. 1. Synthesis schemes of (A) PTX-Cys, PTX-SS-Val and (B) PTX-SS-COOH.

was finally obtained. The yield was 43.57%. The ^{1}H NMR and FT-IR spectra of PTX-SS-Val were shown in Figs. 2C and 3C. In the ^{1}H NMR spectrum of PTX-SS-Val (Fig. 2C), the hydrogen proton peaks attributed to PTX benzene ring appeared at 7.0–8.0 ppm and the dimethyl characteristic absorption of valine appeared at 0.95–1.00 ppm. In addition, compared with the FT-IR spectrum of PTX-Cys, an obvious stretching vibration absorption peak of N-H appeared at 3442.16 cm^{-1} in Fig. 3C, and the characteristic absorption of PTX appeared at 705.68 cm^{-1}. The above results indicated the successful synthesis of PTX-SS-Val.

For PTX-SS-COOH, as shown in Fig. 2D, the hydrogen proton peaks attributed to PTX benzene ring appeared at 7.0–8.0 ppm. Moreover, a new single peak appeared at 12.4 ppm, which was the carboxyl proton absorption peak in PTX-SS-COOH. The result of FT-IR was consistent with that of ^{1}H NMR. As shown in Fig. 3D, the broad absorption peak at 2800-3500 cm^{-1} was the stretching absorption of -COOH, while there was no such absorption peak in the PTX spectrum. Furthermore, the $[M - H]^+$ ion peak at *m/z* 1044.09 of PTX-SS-COOH was confirmed by MS (Fig. S3B). To sum up, PTX-SS-COOH was successfully synthesized.

3.2. Preparation and characterization of PTX prodrug nanoparticles

The PTX prodrug nanoparticles were prepared with nanoprecipitation method. Morphological observations of PTX-Cys, PTX-SS-Val and PTX-SS-COOH prodrug nanoparticles were performed under TEM. As shown in Fig. 4A, the nanoparticles were spherical in shape. Particle size distribution of the nanoparticles, measured by DLS (Fig. 4B), showed that the mean sizes of PTX-Cys, PTX-SS-Val and PTX-SS-COOH nanoparticles were around 213.57 ± 97.40 nm, 131.00 ± 32.30 nm and 126.57 ± 35.20 nm, and the size distribution exhibited a unimodal pattern. These results indicated that the prodrugs could self-assemble into nanoparticles in aqueous solution and improved the solubility of PTX [32].

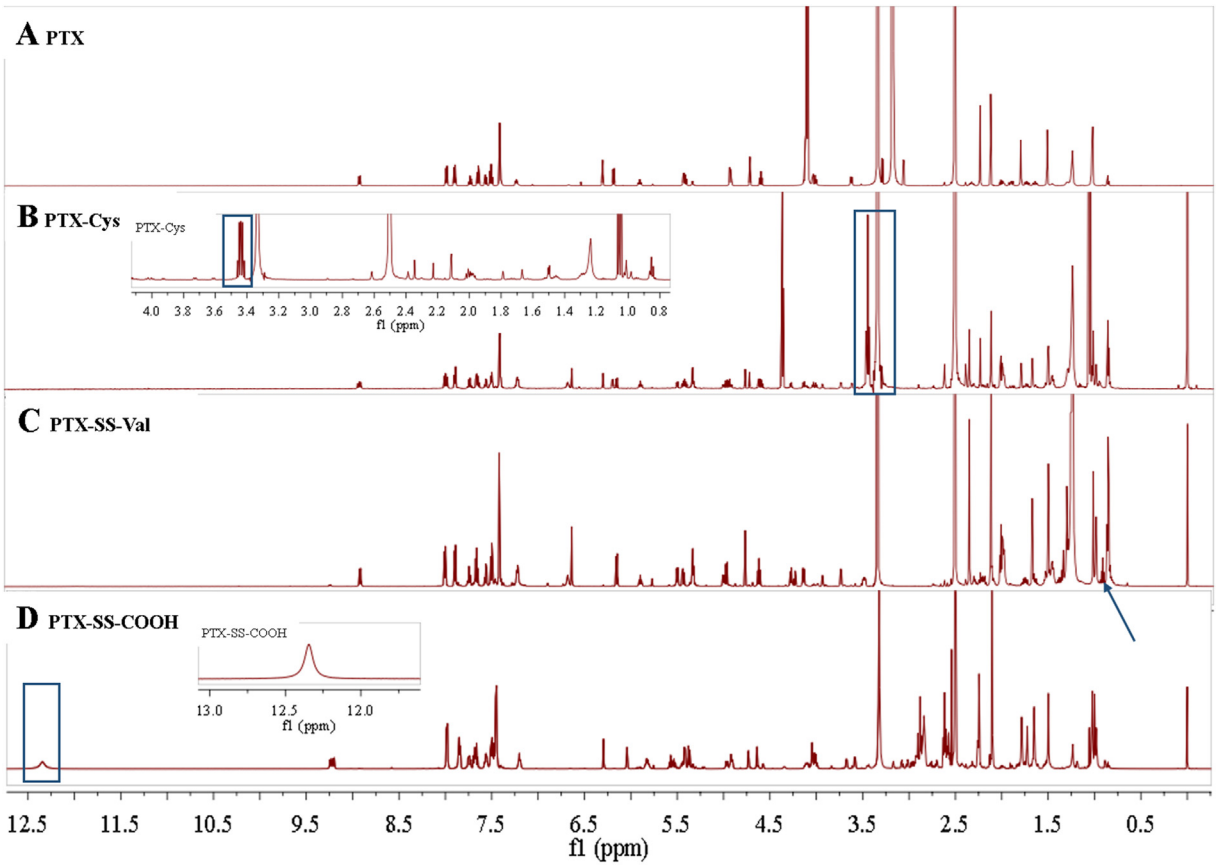

Fig. 2. The ^{1}H NMR spectra of PTX (A), PTX-Cys (B), PTX-SS-Val (C) and PTX-SS-COOH (D) in DMSO-d_6.

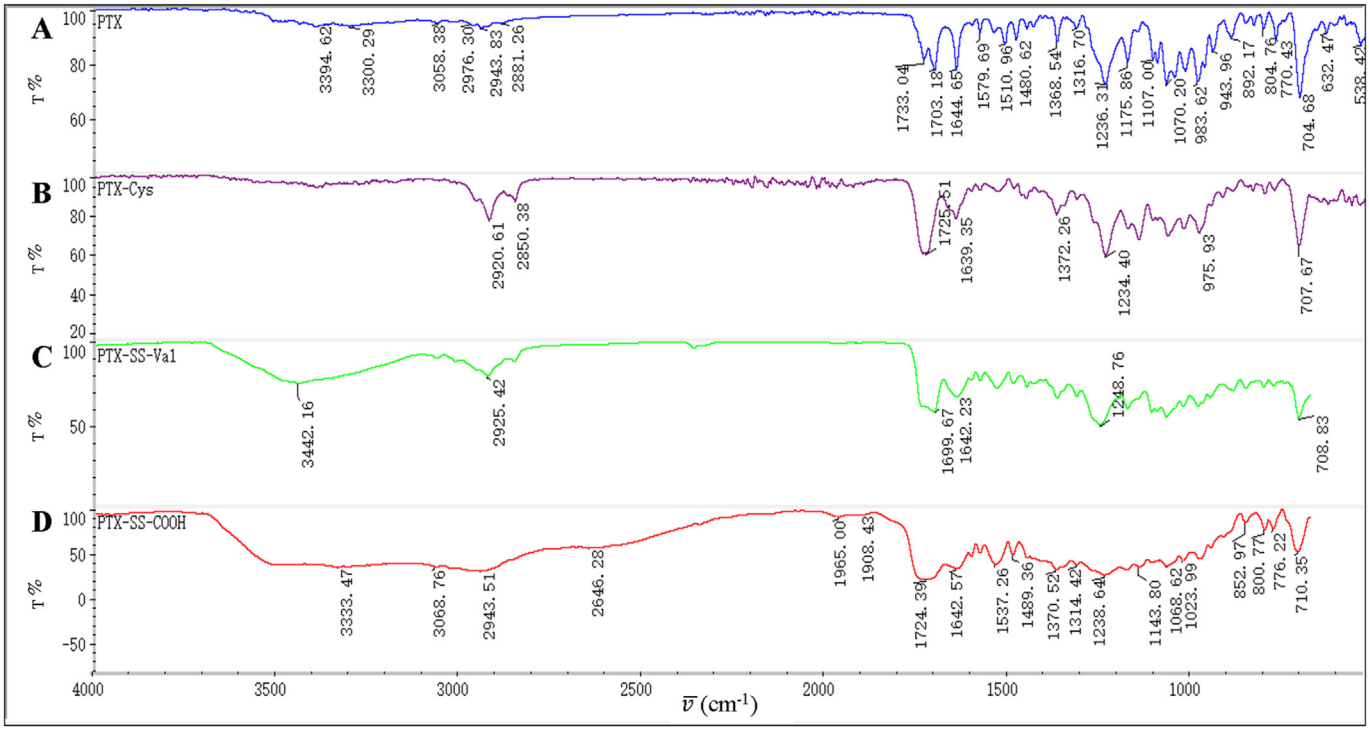

Fig. 3. The FT-IR spectra of PTX (A), PTX-Cys (B), PTX-SS-Val (C) and PTX-SS-COOH (D).

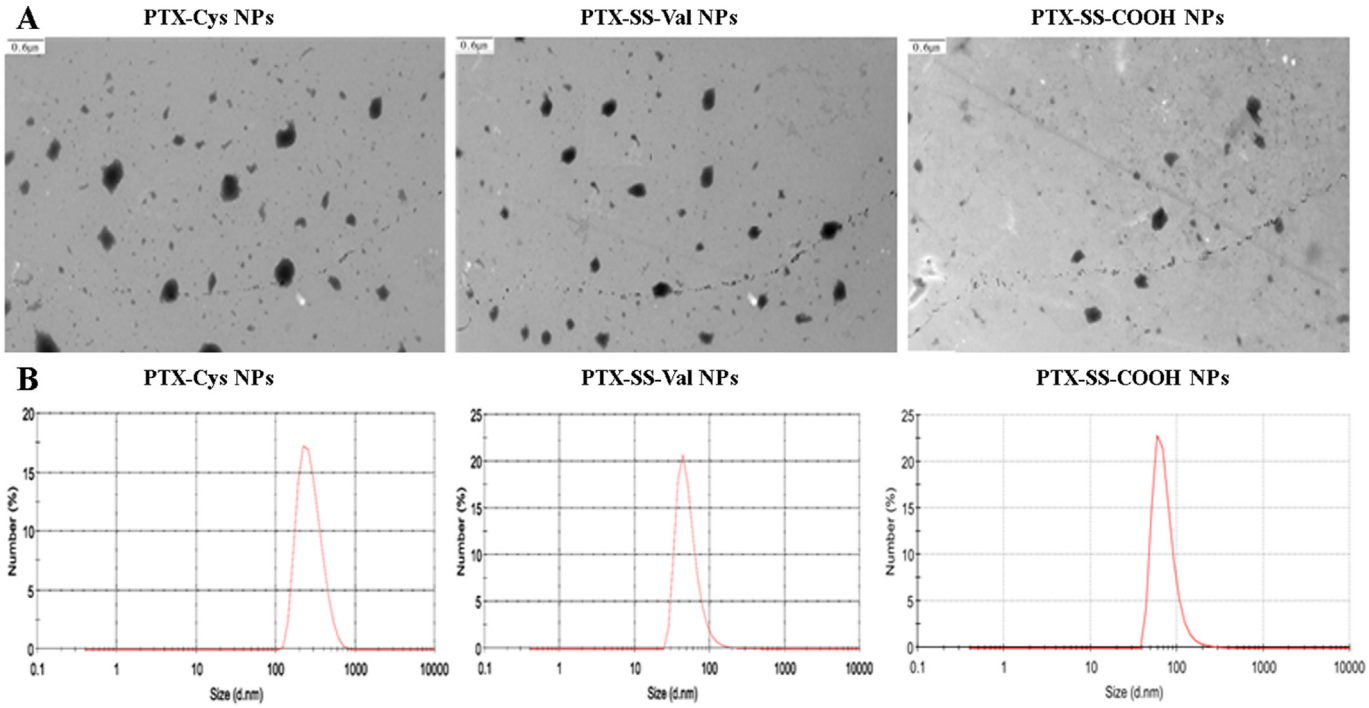

Fig. 4. (A) The TEM images of nanoparticles (the scale bar: 0.6 μm). (B) The size distribution of nanoparticles.

3.3. *In vitro* stability of PTX prodrugs

The chemical stability of PTX prodrugs in buffer solutions of pH 6.5 and pH 7.4 was investigated by dialysis bag method, and expressed as the cumulative release rate of PTX. The cumulative release results of PTX were shown in Fig. S4A&B. After 120 h, the cumulative release of PTX from PTX prodrug was less than 15% in pH 6.5 buffer solution and less than 12% in pH 7.4 buffer solution. Overall, more than 85% of prodrugs kept prototype, indicating the good stability in buffer solutions. However, when 10 mM DTT was present, the *in vitro* cumulative release of PTX for three prodrugs in pH 6.5 buffer solution was significantly accelerated and up to 50%, 58% and 48% was released respectively, exhibiting the redox sensitivity due to presence of the disulfide bond (Fig. S4C).

A severe difficulty encountered with prodrug nanoparticles after oral administration is their instability in the complex gastrointestinal environment. The stability of PTX prodrugs in simulated gastric (SGF) and intestinal fluid (SIF) was investigated by dialysis bag method and expressed as the cumulative release rate of PTX (Fig. S4D&E). SGF containing 0.32% (w/v) pepsin and SIF containing 1% trypsin were used as release medium respectively. Less than 1.5% of PTX released from PTX prodrugs after 4 h in SGF. Meanwhile, in SIF containing trypsin, less than 3.5% of PTX released from PTX prodrugs after 12 h. These results showed that the structure of PTX prodrugs was less affected by pepsin and trypsin, and had good stability in SGF and SIF. It was deduced that after oral administration, the PTX prodrugs could be absorbed by small intestinal epithelial cells with intact structure, which could greatly improve the oral bioavailability of PTX.

3.4. *Cytotoxicity experiments*

Tumor inhibition efficiency of PTX prodrugs was characterized with MTT assay and the Taxol® and PTX solution in DMSO were used as control. The results (Fig. 5) showed that when the drug concentration was increased, the tumor inhibition efficiency was increased, revealing a dose-dependent inhibition behavior. More importantly, the tumor inhibition efficiency of PTX-Cys was significantly higher than other groups, which may be due to the permeability enhancement induced by positively charged amino group which mediated trans-membrane delivery of PTX-Cys.

The cytotoxicity of Taxol® was obviously enhanced with the increase of concentration, because polyoxyethylene castor oil and ethanol in the formulation of Taxol® also had certain cytotoxicity [33]. The cytotoxicity of PTX-SS-Val was greater than that of free PTX when the drug concentration was less than 1 μg/mL, which may be mediated by the transporter PEPT1 overexpressed on the surface of cancer cells [34]. When the drug concentration was greater than 5 μg/mL, the cytotoxicity of PTX-SS-Val was slightly weaker than that of free PTX. It was speculated that the release rate of PTX from PTX-SS-Val molecule was slow, so the cytotoxicity of PTX-SS-Val was slightly weaker than that of free PTX at high concentrations. Finally, PTX-SS-COOH showed the lowest cytotoxicity, which was attributed to the slow release of PTX from PTX-SS-COOH and negative charged carboxyl group which delayed the trans-membrane delivery.

Most of the small molecule prodrugs have been designed to overcome paclitaxel's low water solubility or increase the targeting ability of paclitaxel. Although the prodrugs developed have shown to improve their water solubility or enhanced targeting ability, this has yielded compounds with decreased cytotoxicity, which could be attributable to the inefficient release of paclitaxel from these compounds or poor cell uptake or intracellular process caused by high hydrophilicity [35]. To overcome this problem, PTX-Cys and PTX-SS-Val containing disulfide bonds were developed. The disulfide bonds could be degraded in highly reductive tumor micro or intracellular environment of tumor to promote the PTX release in tumor tissues. The cytotoxicity of PTX-Cys was significantly higher than the PTX solution, which may be due to the permeability enhancement induced by positively charged amino group which mediated trans-membrane delivery of PTX-Cys. PTX-SS-Val exhibited nearly equal anticancer activity to the PTX solution,

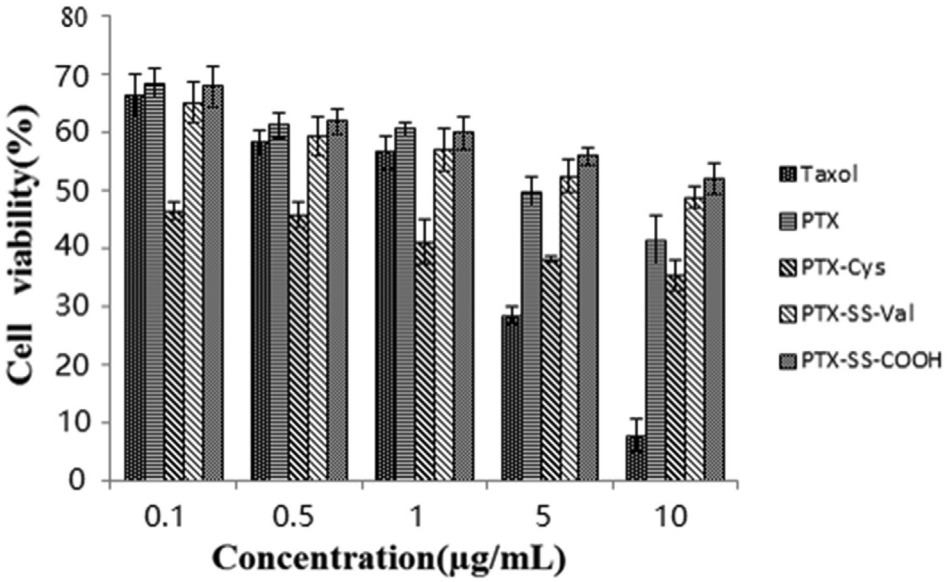

Fig. 5. The *in vitro* anticancer activity of PTX and PTX prodrugs.

perhaps due to the permeability enhancement mediated by PEPT1 transporter. The results demonstrated that PTX-Cys and PTX-SS-Val could be used as potential candidates for anti-tumor drugs.

3.5. Cell uptake experiments

The cellular uptake behavior of C6 loaded PTX-Cys, PTX-SS-Val and PTX-SS-COOH nanoparticles was investigated by a fluorescent inverted microscope (Fig. 6). MCF-7 cells were treated with C6 solution, C6 loaded PTX prodrug nanoparticles for 4 h. As shown in Fig. 6, the green fluorescence (C6 fluorescence) of the nanoparticles was uniformly dispersed around the blue fluorescence (DAPI stained cell nucleus), indicating that the nanoparticles were dispersed in the cytoplasm of MCF-7 cells. The ability of cells to uptake prodrugs could also be evaluated according to the fluorescence intensity. The results showed that after 4 h incubation, the

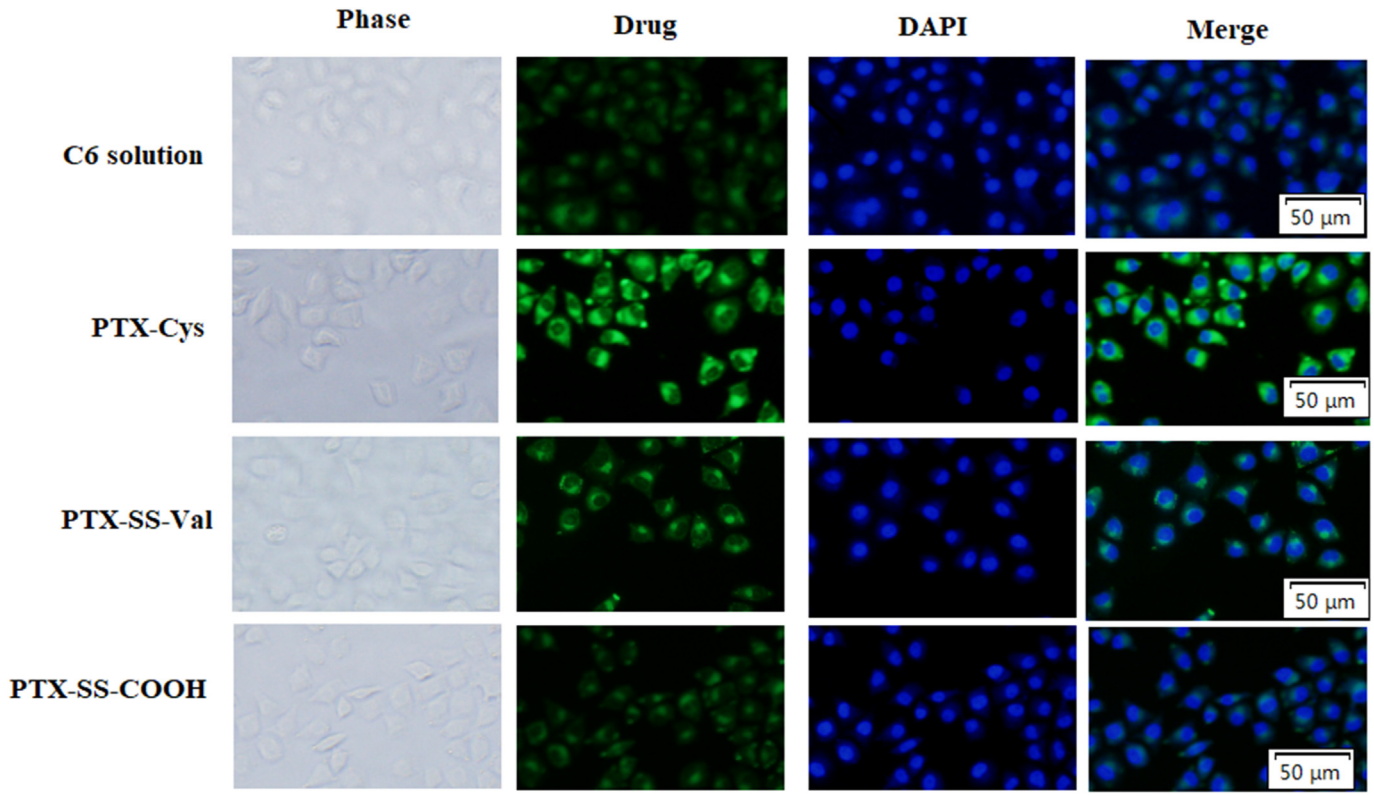

Fig. 6. The cellular uptake of C6 solution and C6 loaded prodrugs after 4 h.

fluorescence intensity of PTX-Cys and PTX-SS-Val groups was stronger than that of C6 solution group and PTX-SS-COOH group, indicating that these two kinds of prodrug nanoparticles were more conducive to cell absorption. More importantly, the cell uptake of PTX-Cys group was the highest, which provided evidence for enhanced tumor permeability of PTX-Cys induced by positively charged amino group which mediated trans-membrane delivery. Furthermore, the fluorescence intensity of PTX-SS-Val group was greater than that of C6 solution and PTX-SS-COOH, which perhaps due to the mediation of PEPT1 transporter.

3.6. Cell apoptosis analysis

The fluorescence microscope and flow cytometer were used to estimate the apoptosis-inducing capabilities of the nanoparticles. As shown in Fig. 7A, after incubating with the formulation group for 48 h, the nuclei of the control group showed uniform blue fluorescence after DAPI staining, with smooth surface and complete structure, while the nuclei of cells treated with prodrug formulations showed different degrees of nucleus rupture and shrinkage. The above experimental results indicated that the PTX-Cys, PTX-SS-Val and PTX-SS-COOH prodrugs uptake by cells could release paclitaxel and induce cell apoptosis. The cell apoptosis was further quantified by flow cytometry using AnnexinV-FITC/PI apoptosis detection kit. As shown in Fig. 7B, the proportion of viable cells was about 100% in the untreated control group. After 48 h of treatment with PTX, PTX-Cys, PTX-SS-Val and PTX-SS-COOH, the proportion of viable cells decreased significantly to, 14.9%, 6.93%, 7.69% and 19.7% respectively, and the proportion of late apoptotic cells was 70.2%, 85.8%, 84.8% and 59.6%, respectively. Compared with the PTX, PTX-SS-Val and PTX-SS-COOH group, the PTX-Cys group induced the largest proportion of apoptosis, which could be due to the enhanced tumor permeability caused by charge characteristics of PTX-Cys. In addition, the apoptosis proportion of the PTX-SS-Val group was greater than that of the free PTX group and PTX-SS-COOH group, demonstrating the enhanced tumor permeability of PTX-SS-Val caused by the mediation effect of PEPT1 transporter. These results were consistent with the results of cytotoxicity and cell uptake *in vitro*. Thus in next animal experiments, the PTX-Cys and PTX-SS-Val prodrugs were used as model drugs to evaluate the potential for improving the oral bioavailability of PTX.

3.7. The absorption of PTX prodrugs in the intestine

The *in vitro* cellular evaluation results showed that PTX-Cys and PTX-SS-Val prodrugs had the superior cytotoxicity and

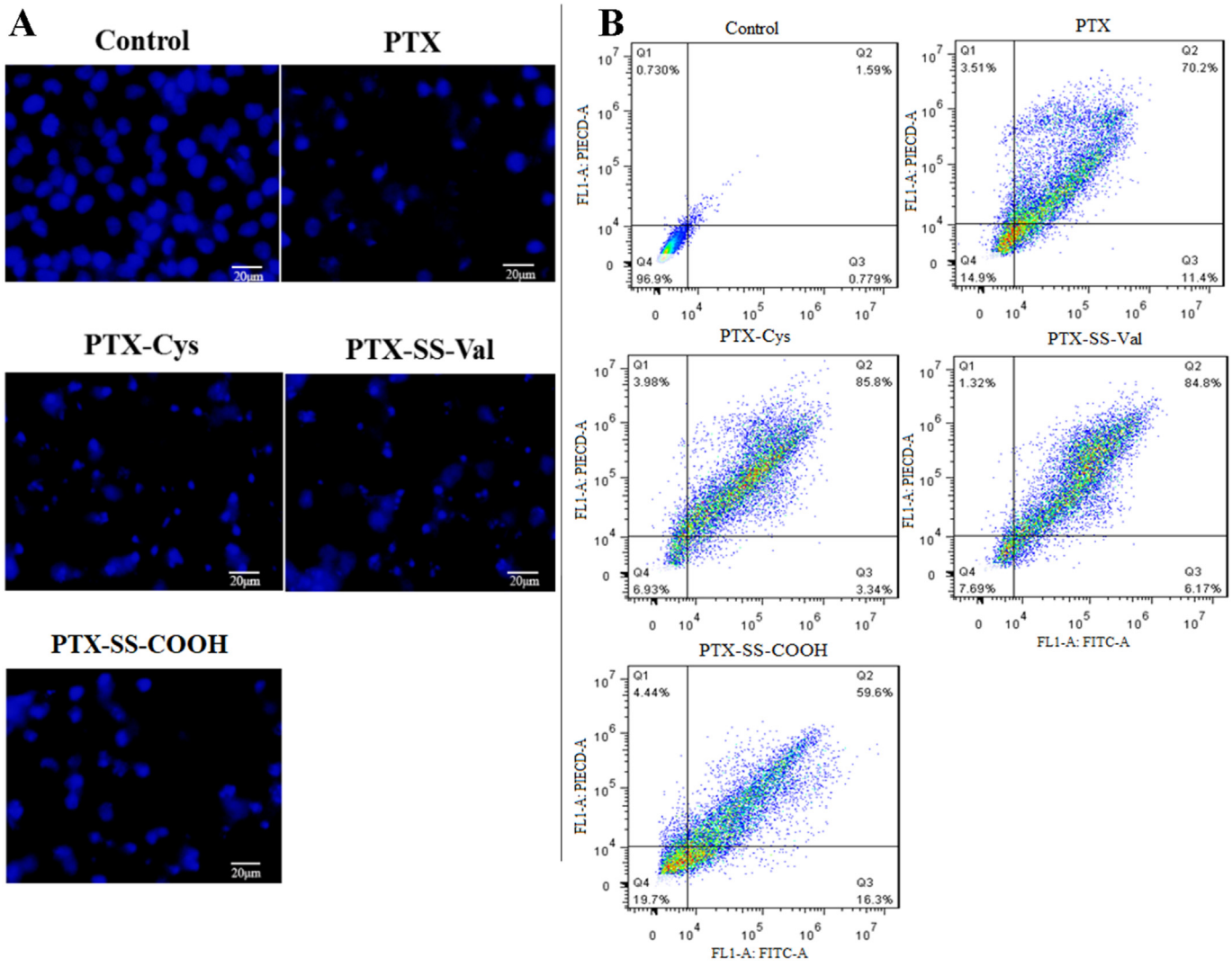

Fig. 7. (A) The cell apoptosis status of MCF-7 cells. (B) The Annexin V/PI assay on MCF-7 cells.

permeability *in vitro*. Thus in next animal experiments, the PTX-Cys and PTX-SS-Val prodrugs were used as model drugs to evaluate the potential for improving the oral bioavailability of PTX.

3.7.1. Effect of different pH perfusates on intestinal absorption

PTX, PTX-Cys and PTX-SS-Val were co-perfused with the two pH perfusates, respectively. It could be seen that intestinal absorption of PTX-Cys and PTX-SS-Val in both perfusates was stronger than that of free PTX (Fig. 8A, Table S1). The P_{eff} of PTX-Cys and PTX-SS-Val in MES (pH 6.5) perfusate was 1.65 and 2.09 times of free PTX, respectively. In HEPES (pH 7.4) perfusate, the P_{eff} of PTX-Cys and PTX-SS-Val was 2.02 and 2.37 times of free PTX, respectively, indicating that the permeability of the prodrugs was greatly improved. The average P_{eff} of PTX-Cys and PTX-SS-Val in HEPES perfusate was 1.31 and 1.21 times than that in MES perfusate, respectively, suggesting that neutral conditions were also conducive to the absorption of prodrugs by small intestinal epithelial cells. This indicated that the targeted transport of PEPT1 was not proton dependent and its transport efficiency was more dependent on the structure of the substrates under neutral conditions.

Compared with PTX-Cys, the average P_{eff} of PTX-SS-Val in MES and HEPES perfusate was 1.27 and 1.17 times than that of PTX-Cys respectively, but the difference was not significant. This phenomenon was presumably due to the transport of PTX-SS-Val mediated by PEPT1 highly expressed in jejunum. In addition, the electrostatic interaction of PTX-Cys with the negative intestinal epithelial cells also promoted the permeation across the intestinal wall, as reported in previous studies [36], which improved its ability to enter small intestinal epithelial cells.

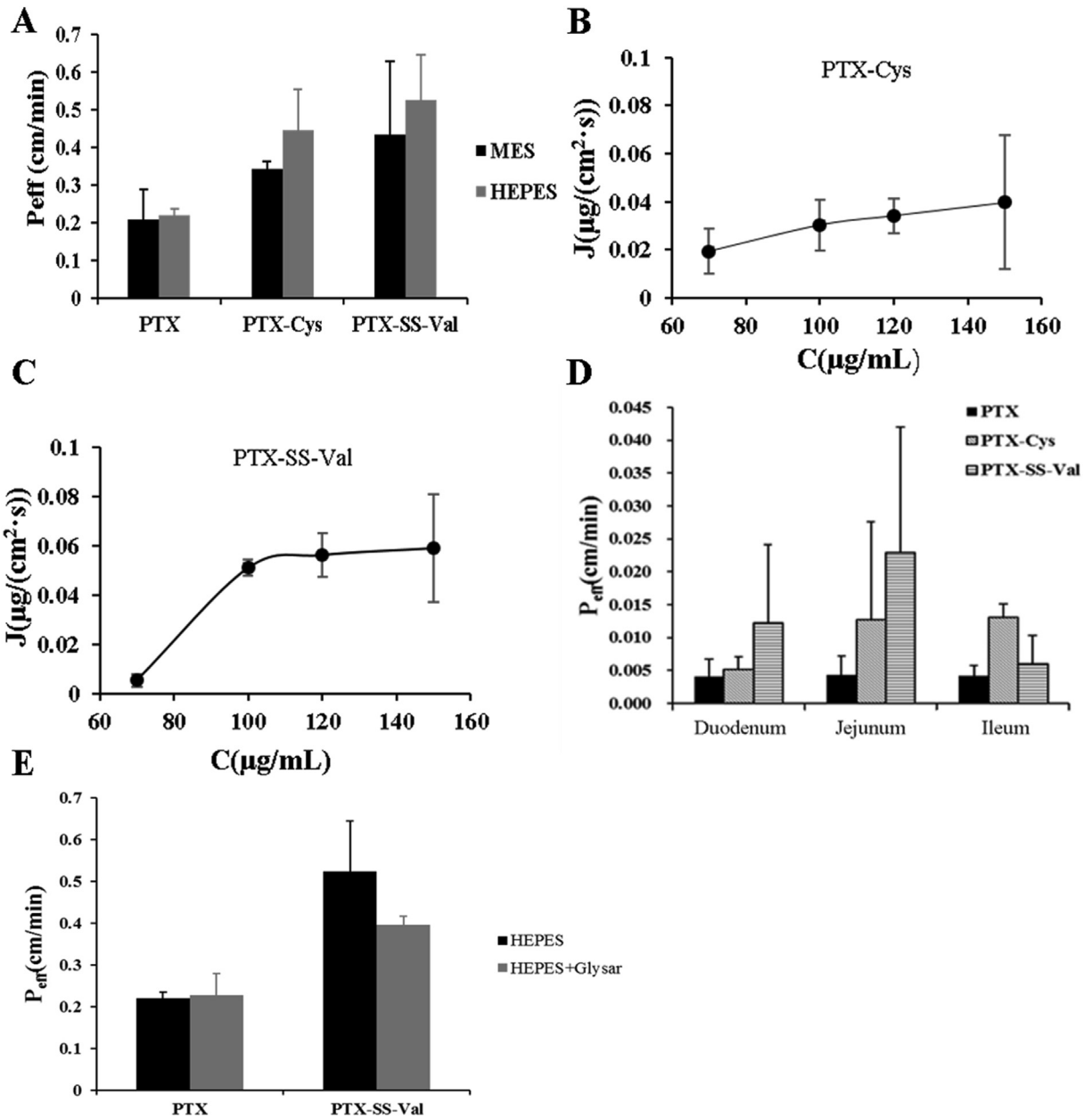

Fig. 8. (A) The P_{eff} of PTX、PTX-Cys and PTX-SS-Val in MES and HEPES solution. The *J* of PTX-Cys (B) and PTX-SS-Val (C) in intestinal circulation at different concentrations. (D) The P_{eff} of PTX and its prodrugs in different intestinal segments.(E) The P_{eff} of PTX and PTX-SS-Val in HEPES ± Gly-Sar solution.

3.7.2. Effect of different drug concentrations on intestinal absorption

To investigate the effect of drug concentration on small intestinal absorption, different concentration gradients of PTX-Cys and PTX-SS-Val were established, and the results of single-pass intestinal perfusion (SPIP) were shown in Table S2&3 and Fig. 8B&C. It could be seen from Fig. 8B that in the range of 70–150 μg/mL, with the increase of concentration, the absorption of PTX-Cys in the small intestine increased continually and there was no apparent transport saturation phenomenon. The P_{eff} did not show obvious differences under different drug concentrations, which showed first-order kinetic absorption characteristics suggesting that passive diffusion mechanism played a major role in intestine absorption. However, for PTX-SS-Val prodrug (Fig. 8C), with the increase of concentration, intestinal absorption began to increase, and then gradually reached a stable state, showing a different absorption mechanism from PTX-Cys. It is speculated that the PEPT1 transporter mediating transport of PTX-SS-Val gradually reached saturation with the increase of concentration, which made the absorption of PTX-SS-Val tend to be flat.

3.7.3. The absorption of PTX prodrugs in different intestinal segments

The absorption of PTX, PTX-Cys and PTX-SS-Val in jejunum, ileum and duodenum was also carried out. The results (Fig. 8D) showed that PTX, PTX-Cys and PTX-SS-Val could be effectively absorbed in different intestinal segments. Compared with other intestinal segments, PTX-SS-Val had the best absorption in the jejunum, though difference was not significant compared with PTX-Cys, which further proved that the transport mediated by transporter PEPT1 promoted the absorption of PTX-SS-Val. However, in other two segments the prodrugs had the similar absorption efficiency especially for PTX-Cys and PTX-SS-Val, because the standard deviations did not show significant differences. The main reason for PTX-Cys was that the electrostatic interaction of PTX-Cys with the negative intestinal epithelial cells promoted the drug absorption in intestinal segments especially in ileum. In addition organic cationic transporter perhaps played a limited role in promoting the absorption of PTX-Cys [37].

3.7.4. Investigation of the effect of PEPT1 inhibition on PTX-SS-Val transport

The results of single-pass intestinal perfusion (SPIP) of PTX and PTX-SS-Val in HEPES solution with or without Gly-Sar were shown in Fig. 8E. From the above experimental results, it could be seen that the intestinal absorption capacity of free PTX in HEPES solution was not significantly different with or without Gly-Sar, while the P_{eff} of PTX-SS-Val in HEPES solution was 1.59 and 1.3 times higher than that in HEPES + Gly-Sar solution, indicating that there was a binding competition between PTX-SS-Val and Gly-Sar for PEPT1 transporter. Gly-Sar could bind with part of the transporters and inhibit the absorption of PTX-SS-Val in small intestine. This provided further evidence that PEPT1 transporter involved the absorption of PTX-SS-Val in small intestine.

In general, PTX-SS-Val and PTX-Cys had a similar absorption in intestine. This phenomenon was mainly due to the different transport mechanisms. The transport of PTX-SS-Val mediated by PEPT1 highly expressed in jejunum promoted the absorption of drug in intestine. The electrostatic interaction of PTX-Cys with the negative intestinal epithelial cells also promoted the permeation across the intestinal wall of drug. However, since most normal cells are negatively charged, positively charged compounds often have a strong side effect. Thus in the next pharmacokinetic experiment, the PTX-SS-Val was used as model drugs to evaluate the potential for improving the oral bioavailability of PTX.

3.8. Oral pharmacokinetics of PTX prodrugs

3.8.1. Tissue accumulation following in situ intestinal perfusion

To assess the metabolism of PTX prodrug in intestinal tissue, the contents of PTX prodrug and PTX in the intestinal tissue were determined after the concentration-dependent perfusion experiment. The results showed that 2 h after intestinal perfusion, for PTX-Cys prodrug, in intestinal tissue, about 42% of drugs existed in the form of PTX-Cys molecule, about 58% of drugs existed in the form of PTX. While for PTX-SS-Val, about 22% of drugs existed in the form of PTX-SS-Val, about 78% of drugs existed in the form of PTX. The low concentration of prodrug and high concentration of PTX in the intestine homogenate indicated that the prodrug was hydrolyzed partly within the enterocytes via an intestinal first-pass effect.

3.8.2. Oral pharmacokinetics evaluation

As the prodrugs would be partly transformed into PTX via the intestinal first-pass effect, therefore, the drug concentration in plasma was determined through hydrolyzing the prodrug to measure the whole PTX (free and hydrolyzed PTX) and calculated the pharmacokinetic parameters. The pharmacokinetics of PTX formulations under different routes of administration were analyzed by DAS2.0 software, and the results were shown in Table 1. Plasma concentration-time profiles of PTX following administration of different PTX formulations were shown in Fig. 9. According to the pharmacokinetic parameters, after 24 h of intragastric administration, the AUC of Taxol® group was 15.051 mg/L*h, while that of PTX-SS-Val group was 23.863 mg/L*h, which was 1.56 times higher than that of Taxol® group. The C_{max} of PTX-SS-Val group was 1.2383 mg/L, which was significantly higher than that of Taxol® group, and the absolute bioavailability (F) increased from 19.31% to 30.61%. This phenomenon could be explained by the improved water solubility of drugs and the transport of PTX-SS-Val mediated by the transporter PEPT1, which significantly promoted the absorption of PTX-SS-Val and significantly enhanced the oral bioavailability of PTX. The clearance of PTX-SS-Val (0.838 L/h/kg) was about 1.6 times less that of Taxol® (1.329 L/h/kg). The main reason for this was that the high water solubility of PTX-SS-Val made it more likely to stay in the blood stream.

4. Conclusion

In this study, the hydrophobic antitumor drug paclitaxel was chemically modified and a series of novel amphiphilic paclitaxel small molecule prodrugs, PTX-Cys, PTX-SS-Val and PTX-SS-COOH were designed, synthesized and evaluated against cancer cell lines. These prodrugs contain water-soluble groups such as amino, carboxyl and amino acids to increase the aqueous solubility of prodrugs when compared to paclitaxel. More importantly, the valine was introduced in molecule of PTX-SS-Val and made the

Table 1
The pharmacokinetic parameters of different PTX formulations.

Parameters	Unit	Taxol[a]	Taxol[b]	PTX-SS-Val[b]
$AUC_{(0-\infty)}$	mg/L*h	18.709	15.051	23.863
$MRT_{(0-\infty)}$	h	11.724	16.94	19.27
T_{max}	h	0.25	4	2
V_z	L/kg	11.355	19.258	15.769
CL_z	L/h/kg	1.069	1.329	0.838
C_{max}	mg/L	6.0650	1.062	1.2383
F (%)			19.31	30.61

[a] Intravenous administration.
[b] Intragastric administration.

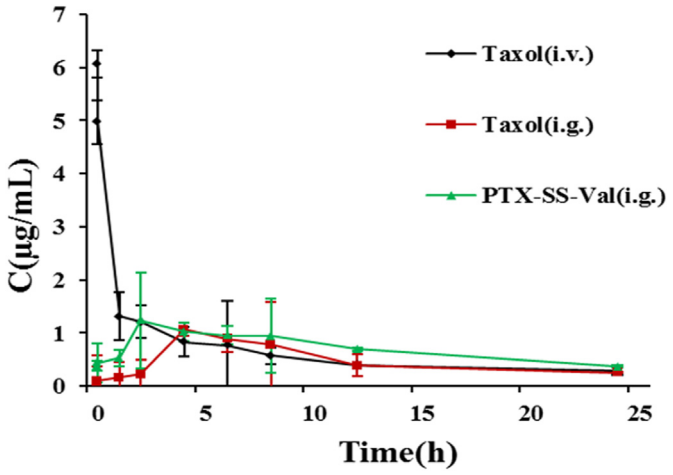

Fig. 9. Plasma concentration-time profiles of PTX following administration of different PTX formulations.

molecule conform to the structural characteristics of intestinal oligopeptide transporter PEPT1 substrate. Thus oral bioavailability of prodrug could be improved because of the mediation of PEPT1 transporter. These small molecule paclitaxel prodrugs could self-assemble into nanoparticles in aqueous solution, which could effectively improve the solubility of paclitaxel, and had certain stability in pH 6.5, pH 7.4 buffer solutions and simulated gastrointestinal fluids. Among them, PTX-Cys and PTX-SS-Val exhibited equal or better anticancer activity when compared to that of paclitaxel. The single-pass intestinal perfusion (SPIP) experiments in the rat demonstrated that PTX-Cys, PTX-SS-Val had higher intestinal absorption capacity than free paclitaxel. Oral pharmacokinetic experiments showed that PTX-SS-Val could effectively improve the oral bioavailability of paclitaxel. With our work, we developed an efficient paclitaxel prodrug, with great potential to be administered orally, overcoming drawbacks of the pharmacokinetic profile of this lipophilic natural product.

Submission declaration and verification

This work has not been published previously. It is not under consideration for publication elsewhere. Its publication is approved by all authors and tacitly or explicitly by the responsible authorities where the work was carried out. If accepted, it will not be published elsewhere in the same form, in English or in any other language, including electronically without the written consent of the copyright-hold.

Declaration of competing interest

The authors declare that they have no known competing financial interests or personal relationships that could have appeared to influence the work reported in this paper.

Acknowledgements

This work was financially supported by the Key Research and Development Program of Shandong Province (grant numbers 2018CXGC1411), Natural Science Foundation for Young Scholars of China (grant number 81503261) and the Natural Science Foundation of Shandong Province (grant number ZR2015HM070).

Appendix A. Supplementary data

Supplementary data to this article can be found online at https://doi.org/10.1016/j.ejmech.2021.113276.

References

[1] H. Bu, X. He, Z. Zhang, Q. Yin, H. Yu, Y. Li, A TPGS-incorporating nanoemulsion of paclitaxel circumvents drug resistance in breast cancer, Int. J. Pharm. 471 (2014) 206–213, https://doi.org/10.1016/j.ijpharm.2014.05.039.
[2] E. Bernabeu, L. Gonzalez, M. Cagel, et al., Novel Soluplus®-TPGS mixed micelles for encapsulation of paclitaxel with enhanced in vitro cytotoxicity on breast and ovarian cancer cell lines, Colloids Surf., B 140 (2016) 403–411, https://doi.org/10.1016/j.colsurfb.2016.01.003.
[3] M. Skwarczynski, et al., Paclitaxel Prodrugs: toward smarter delivery of anticancer agents, J. Med. Chem. 49 (2006) 7253–7269.
[4] R. Mo, X. Jin, N. Li, C. Ju, M. Sun, et al., The mechanism of enhancement on oral absorption of paclitaxel by N-octyl-O-sulfate chitosan micelles, Biomaterials 32 (2011) 4609–4620, https://doi.org/10.1016/j.biomaterials.2011.03.005.
[5] X. Du, A.R. Khan, M. Fu, J. Ji, et al., Current development in the formulations of non-injection administration of paclitaxel, Int. J. Pharm. 542 (2018) 242–252, https://doi.org/10.1016/j.ijpharm.2018.03.030.
[7] Z. Wang, D. Chi, X. Wu, Y. Wang, X. Lin, Z. Xu, et al., Tyrosine modified irinotecan-loaded liposomes capable of simultaneously targeting LAT1 and $ATB^{0,+}$ for efficient tumor therapy, J. Contr. Release 316 (2019) 22–33, https://doi.org/10.1016/j.jconrel.2019.10.037.
[6] Q. Jiang, J. Zhang, P. Tong, Y. Gao, Y. Lv, C. Wang, M. Luo, M. Sun, et al., Bioactivatable pseudotripeptidization of cyclic dipeptides to increase the affinity toward oligopeptide transporter 1 for enhanced oral absorption: an application to cyclo(l-hyp-l-ser) (JBP485), J. Med. Chem. 62 (2019) 7708–7721, https://doi.org/10.1021/acs.jmedchem.9b00358.
[8] Y. Sun, J. Sun, S. Shi, et al., Synthesis, transport and pharmacokinetics of 5 '-Amino acid ester prodrugs of 1-β-D-Arabinofuranosylcytosine, Mol. Pharm. 6 (2009) 315–325, https://doi.org/10.1021/mp800200a.
[9] V.T. Banala, S. Urandur, S. Sharma, M. Sharma, R.P. Shukla, D. Marwaha, S. Gautam, M. Dwivedi, P.R. Mishra, Targeted co-delivery of aldose reductase inhibitor epalrestat and chemotherapeutic doxorubicin via redox-sensitive prodrug approach promotes synergistic tumor suppression, Biomater. Sci. 7 (2019) 2889–2906, https://doi.org/10.1039/C9BM00221A.
[10] C. Dong, Q. Zhou, J. Xiang, F. Liu, et al., Self-assembly of oxidation-responsive polyethylene glycol-paclitaxel prodrug for cancer chemotherapy, J. Contr. Release 321 (2020) 529–539, https://doi.org/10.1016/j.jconrel.2020.02.038.
[11] Q. Zhang, P. Zhang, S. Jian, J. Li, F. Li, X. Sun, H. Li, Y. Zeng, et al., Drug-bearing peptide-based nanospheres for the inhibition of metastasis and growthof cancer, Mol. Pharm. 17 (2020) 3165–3176, https://doi.org/10.1021/acs.molpharmaceut.0c00118.
[12] D. Ye, A.J. Shuhendler, L. Cui, et al., Bioorthogonal cyclization-mediated in situ self-assembly of small-molecule probes for imaging caspase activity in vivo, Nat. Chem. 6 (2014) 519–526, https://doi.org/10.1038/nchem.1920.
[13] Y. Cheng, Y. Ji, Mitochondria-targeting nanomedicine self-assembled from GSH-responsive paclitaxel-ss-berberine conjugate for synergetic cancer treatment with enhanced cytotoxicity, J. Contr. Release 318 (2020) 38–49, https://doi.org/10.1016/j.jconrel.2019.12.011.
[14] H. Wang, X. Liu, Y. Wang, Y. Chen, Q. Jin, J. Ji, Doxorubicin conjugated phospholipid prodrugs as smart nanomedicine platforms for cancer therapy, J. Mater. Chem. B 3 (2015) 3297–3305, https://doi.org/10.1039/C4TB01984A.
[15] R.E. Wang, T. Liu, Y. Wang, et al., An immunosuppressive antibody-drug conjugate, J. Am. Chem. Soc. 137 (2015) 3229–3232, https://doi.org/10.1021/jacs.5b00620.
[16] X. Tan, B. Li, X. Lu, et al., Light-triggered, self-immolative nucleic acid-drug nanostructures, J. Am. Chem. Soc. 137 (2015) 6112–6115, https://doi.org/10.1021/jacs.5b00795.
[17] Z. Meng, Q. Lv, et al., Prodrug strategies for paclitaxel, Int. J. Mol. Sci. 17 (2016) 796, https://doi.org/10.3390/ijms17050796.
[18] H. Ren, Y. He, J. Liang, Z. Cheng, M. Zhang, et al., Role of liposome size, surface charge, and PEGylation on rheumatoid arthritis targeting therapy, ACS Appl. Mater. Interfaces 11 (2019) 20304–20315, https://doi.org/10.1021/acsami.8b22693.
[19] Z. Zhang, L. Mei, et al., Paclitaxel drug delivery systems, Expert Opin, Drug Deliv. 10 (2013) 325–340, https://doi.org/10.1517/17425247.2013.752354.
[20] N. Zisman, S.N. Dos, S. Johnstone, A. Tsang, D. Bermudes, et al., Optimizing liposomal Cisplatin efficacy through membrane composition manipulations, Chemother. Res. Pract. 2011 (1–7) (2011), 213848, https://doi.org/10.1155/2011/213848.
[21] Y. Li, Y.H. Li, W. Ji, Z. Lu, L. Liu, Y. Shi, G. Ma, X. Zhang, Positively charged polyprodrug amphiphiles with enhanced drug loading and reactive oxygen species-responsive release ability for traceable synergistic therapy, J. Am. Chem. Soc. 40 (2018) 4164–4171, https://doi.org/10.1021/jacs.8b01641.
[22] Q. Zhou, S. Shao, J. Wang, C. Xu, J. Xiang, Y. Piao, et al., Enzyme-activatable polymer–drug conjugate augments tumour penetration and treatment efficacy, Nat. Nanotechnol. 14 (2019) 799–809, https://doi.org/10.1038/s41565-019-0485-z.
[23] L. Zhou, H. Wang, Y. Li, Stimuli-responsive nanomedicines for overcoming

cancer multidrug resistance, Theranostics 8 (2018) 1059–1074. https://www.thno.org/v08p1059.htm.
[24] X. Deng, et al., Discovery of novel cell-penetrating and tumor-targeting peptide-drug conjugate (PDC) for programmable delivery of paclitaxel and cancer treatment, Eur. J. Med. Chem. 27 (2020) 113050, https://doi.org/10.1016/j.ejmech.2020.113050.
[25] H. Gao, Z. Hu, Q. Guan, et al., Synthesis and thermoreversible gelation of coil-helical polyethylene-block-poly(γ-benzyl-l-glutamate) diblock copolymer, Polymer 54 (2013) 4923–4929, https://doi.org/10.1016/j.polymer.2013.06.055.
[26] Y. Liu, J. Sun, W. Cao, J. Yang, H. Lian, X. Li, Y. Sun, Y. Wang, S. Wang, Z. He, Dual targeting folate-conjugated hyaluronic acid polymeric micelles for paclitaxel delivery, Int. J. Pharm. 421 (2011) 160–169, https://doi.org/10.1016/j.ijpharm.2011.09.006.
[27] K. Zhou, Y. Zhu, X. Chen, et al., Redox- and MMP-2-sensitive drug delivery nanoparticles based on gelatin and albumin for tumor targeted delivery of paclitaxel, Mater. Sci. Eng. C 114 (2020), 111006, https://doi.org/10.1016/j.msec.2020.111006.
[28] T. Ren, Q. Wang, Y. Xu, et al., Enhanced oral absorption and anticancer efficacy of cabazitaxel by overcoming intestinal mucus and epithelium barriers using surface polyethylene oxide (PEO) decorated positively charged polymer-lipid hybrid nanoparticles, J. Contr. Release 269 (2017) 423–438, https://doi.org/10.1016/j.jconrel.2017.11.015.
[29] Y. Gao, J. Chen, X. Zhang, et al., Quantification of paclitaxel and polyaspartate paclitaxel conjugate in beagle plasma: application to a pharmacokinetic study, J. Chromatogr. Sci. 55 (2017) 222–231, https://doi.org/10.1093/chromsci/bmw174.
[30] W. Tao, D. Zhao, M. Sun, Z. Wang, B. Lin, Y. Bao, Y. Li, Z. He, Y. Sun, J. Sun, Intestinal absorption and activation of decitabine amino acid ester prodrugs mediated by peptide transporter PEPT1 and enterocyte enzymes, Int. J. Pharm. 541 (2018) 64–71, https://doi.org/10.1016/j.ijpharm.2018.02.033.
[31] M. Gund, A. Khanna, N. Dubashi, et al., Water-soluble prodrugs of paclitaxel containing self-immolative disulfide linkers, Bioorg, Med. Chem. Lett. 25 (2014) 122–127, https://doi.org/10.1016/j.bmcl.2014.10.088.
[32] Y. Hayashi, et al., A novel approach of water-soluble paclitaxel prodrug with No auxiliary and No Byproduct: design and synthesis of isotaxel, J. Med. Chem. 46 (2003) 3782–3784. https://pubs.acs.org/doi/abs/10.1021/jm034112n.
[33] X. Dong, C.A. Mattingly, M.T. Tseng, et al., Doxorubicin and paclitaxel-loaded lipid-based nanoparticles overcome multidrug resistance by inhibiting P-glycoprotein and depleting ATP, Canc. Res. 69 (2009) 3918–3926, https://doi.org/10.1158/0008-5472.CAN-08-2747.
[34] Z. Wang, D. Chi, X. Wu, Y. Wang, X. Lin, Z. Xu, et al., Tyrosine modified irinotecan-loaded liposomes capable of simultaneously targeting LAT1 and $ATB^{0,+}$ for efficient tumor therapy, J. Contr. Release 316 (2019) 22–33, https://doi.org/10.1016/j.jconrel.2019.10.037.
[35] H. Ren, Y. He, J. Liang, Z. Cheng, M. Zhang, et al., Role of liposome size, surface charge, and PEGylation on rheumatoid arthritis targeting therapy, ACS Appl. Mater. Interfaces 11 (2019) 20304–20315, https://doi.org/10.1021/acsami.8b22693.
[36] F.Z. Dahmani, H. Yang, J. Zhou, J. Yao, et al., Enhanced oral bioavailability of paclitaxel in pluronic/LHR mixed polymeric micelles: preparation, *in vitro* and *in vivo* evaluation, Eur. J. Pharmaceut. Sci. 47 (2012) 179–189, https://doi.org/10.1016/j.ejps.2012.05.015.
[37] Z. Wang, D. Chi, X. Wu, Y. Wang, X. Lin, Z. Xu, et al., Tyrosine modified irinotecan-loaded liposomes capable of simultaneously targeting LAT1 and $ATB^{0,+}$ for efficient tumor therapy, J. Contr. Release 316 (2019) 22–33, https://doi.org/10.1016/j.jconrel.2019.10.037.